Defect generation, advanced crystallization, and characterization methods for high-quality solar-cell silicon

Feature Article

Marisa Di Sabatino* and Gaute Stokkan**

Department of Materials Science and Engineering, Norwegian University of Science and Technology (NTNU), A. Getz vei 2B, 7491 Trondheim, Norway

* Corresponding author: e-mail marisa.di.sabatino@material.ntnu.no, Phone: +47 735 51 205, Fax: +47 735 50 203
** e-mail gaute.stokkan@material.ntnu.no, Phone: +47 735 97 089, Fax: +47 735 50 203

Silicon is the dominant material for production of solar cells. Research work constantly aims at improving the quality of the silicon materials to achieve higher solar-cell conversion efficiencies. It has been demonstrated that defects and impurities, often rising during the silicon ingot production and due to the presence of impurity sources throughout the silicon solar-cell value chain (e.g. silicon feedstock, crucible and coating, furnace atmosphere, etc.), have a detrimental effect on device performances. Crystallization is the first step in the solar-cell value chain. During crystallization, crystal defects, such as grain boundaries and dislocations, develop, and impurities, such as dopants and metals, distribute. By controlling the process, we can also control the defect formation and impurity segregation. In this study, we review some of the work carried out at NTNU to understand the role of defects and impurities on materials properties. Specifically, we report on some of the work done on defects, crystallization, and characterization.

1 Introduction There is currently great interest in understanding the influence of impurities and crystal defects in multicrystalline silicon on the electrical properties of solar cells. Multicrystalline silicon is the dominant solar-cell material (56% of world production) [1]. The interacting properties of impurities and crystal defects of this material result in an absolute decrease of the efficiency of such cells of about 2% compared to monocrystalline cells. A recent review of the processes for solar-cell silicon can be found in Ref. [2]. Efforts have been made to produce multicrystalline silicon solar cells, which have lower process cost than the monocrystalline cells, while retaining high material quality and good device performance. The key to utilizing some of the development in solar-cell processing to allow such efficiency increases lies in understanding the effects of impurities, defects, and their interaction, and how these may be controlled by measures taken during production and processing of the material.

Several of the most important material-quality parameters, such as grain boundary type and density, dislocation density, impurity concentration, and chemical state are either completely determined during the crystallization process, or can be altered at later stages of this process or of the solar-cell value chain. Since crystallization processes are fundamental for the formation of microstructure and defects, and hence the final quality of the ingots for the solar cells manufacturing, it has been the topic of many research works in recent decades. In this paper, we will review the recent research work at NTNU on defects, crystallization, and characterization of silicon for high-efficiency solar cells and briefly insert them in the international context.

2 Defects and defect generation The main crystal defects in multicrystalline silicon are: grain boundaries, twins, stacking faults, and dislocations. A brief review of the properties of the various defects, and an overview of the current understanding of their generation will be given, before some specific studies performed at NTNU are reviewed.

Grain boundaries and twins are the crystal defects that can be visually distinguished on a silicon surface, such as a

wafer, since they separate crystallites of different orientation. Grain boundaries can be classified into three categories relating to their degree of symmetry: coincidence site lattice (CSL) type boundaries, low-angle boundaries, and random boundaries. CSL boundaries separate two crystallites where a certain number of lattice points are common to the two, allowing for a higher degree of grain-boundary symmetry and lower energy. The twin is a special case of such a boundary with a particularly high degree of symmetry and consequently low energy. It is generally found that CSL boundaries are less detrimental to electrical properties than other types of grain boundaries, which is also found to correlate with the amount of impurities decorating the boundaries [3]. However, since grain boundaries tend to reconstruct, i.e. chemical bonds are bent and stretched to allow low-energy configurations, there is no simple relation between the apparent degree of symmetry given by the CSL and the grain-boundary energy. The grain-boundary energy also depends on the orientation of the grain boundary relative to the crystals, and if the grain boundary is forced to attain an orientation different from a low-energy position, the grain boundary will split or facet into lower energy configurations [4]. All these factors influence the responsiveness of the grain boundary to impurity decoration and thus their electrical activity.

Random grain boundaries, i.e. separating crystallites without common lattice points, generally have higher electrical activity than CSL boundaries, but their density is very low [5]. A study performed at NTNU indicated that 95% of all grain boundaries are CSL boundaries of some type.

The third type of grain boundary, the subgrain boundary, separates parts of a crystal with very small differences in orientation. They consist of separate dislocations arranged in a planar structure. These grain boundaries are the most important type, both because of their high density compared to random grain boundaries, and because of their high electrical activity, measured by Chen and Sekiguchi [6] to be the highest of all types; electrical activity increases with the difference in orientation between crystallites up to ~2°, to a stable level. This is explained by overlapping dislocation cores (see below on dislocations). Subgrain boundaries are formed during crystal growth or during cooling as a reaction between individual dislocations to lower their common Gibbs free energy, a process referred to as *recovery*.

Dislocations are fundamentally related to plastic deformation of materials, see e.g. Ref. [7]. In silicon plastic deformation, and thus movement and generation of dislocations, appears at high temperature only, as the material is brittle at room temperature. In initially dislocation-free material, dislocations can be generated if the crystal is stressed beyond the elastic limit of the material; this is a very high stress level not achieved during growth or cooling of silicon crystals. Instead, dislocations can appear at stress concentrators, such as grain-boundary kinks, melt impingements, particles of other phases or surfaces. Once initial dislocations exist, they will move when the crystal is stressed, and this can produce new dislocations through the processes of *Frank–Read sources* or *multiple crossglide*, also called *dislocation multiplication*. Frequently, constitutive modelling is used to link expected stress patterns resulting from measured thermal profiles to dislocation density in the material. This is achieved by using the Alexander–Haasen model [8], the validity of which has been verified for stressed single crystal, but is much more challenging for multicrystals. This is due to unknown boundary conditions at grain boundaries and unknown initial conditions (i.e. how many initial dislocations are present before the modelling starts). Modelling reports have been presented by several groups [9–11], and general patterns appear similar to observations on actual material, but details cannot yet be predicted. It is currently not known to what degree the observed dislocation density is a result of generation at stress concentrators, multiplication, or recovery. Traditionally, the multiplication phase has been emphasized, but recent investigations reviewed below indicate that the other two phases should be considered as well.

Dislocations, like grain boundaries, reconstruct to lower their energy, and uncontaminated dislocations are not electrically active [12]. The reason why dislocations are considered the most important defects in multicrystalline silicon today is because of their interaction with impurities. A model developed by Kveder et al. [13] explains why dislocations contaminated by impurities enhance the recombination effect of both species through the large capture cross section of the dislocations, the deep energy level of the contaminants and the transition from one defect to the other by overlapping wave functions. This, combined with the inability to properly getter metals from regions of high dislocation density, explained by Kittler et al. [12] and demonstrated, e.g., by Bentzen et al. [14], cause regions of high dislocation density to be the poorest performing regions of the multicrystalline silicon solar cell.

Another important feature of dislocations in multicrystalline silicon is that the electrical activity varies significantly, even over small distances within the same material. This was demonstrated by Rinio et al. [15] by applying the model of Donolato [16] to the measurements of dislocation density and electrical response. This is believed to be a consequence of different thermal history, but the actual mechanisms are not known, although some suggestions have been given [15, 17].

The nucleation conditions appear to have a large impact on the concentration of dislocations in multicrystalline silicon, which was shown in a study of a series of ingots produced in our pilot-scale directional solidification furnace [18]. Dislocation density was measured using PVScan, and it was generally observed that large variations in dislocation density occurred from ingot to ingot. The dislocation density harmful for solar cell operation ($\sim 10^5 \, \text{cm}^{-3}$) covered 30–40% of the wafer area in one class of ingots (labelled *high dislocation density*) whereas in another class it was as low as 10–20% (*low dislocation density*).

Phys. Status Solidi A 210, No. 4 (2013)

643

These observations were compared to EBSD measurements, which showed that large grains occurred in the bottom of low and high density dislocation ingots alike, and both types could be seen to result from nucleation on dendrites grown in ⟨112⟩ or ⟨110⟩ direction, similar to the work of Fujiwara et al. [19], explained in the next section on crystallization processes. However, it was clear that these dendrites had not necessarily grown exactly parallel to the crucible bottom, as in the case of Ref. [19], and a correlation was observed between low and high angles between the dendrites and the crucible bottom, and low and high dislocation density, respectively. When comparison was made to the power consumption during the nucleation event for these ingots, it was observed that the low-angle, low dislocation density ingots exhibited a sharp release of heat directly after nucleation, whereas the others showed a more gradual release of heat. This clearly corresponds to fast dendritic growth in a shallow volume close to the crucible bottom and to more time-consuming growth in a thicker volume, prior to the start of directional solidification. The conclusion from this study is that in order for dendritic nucleation and structure control to have a positive impact on dislocation density, supercooling conditions need to be controlled such that only a shallow volume close to the crucible bottom is affected.

Although some prerequisites for growing low dislocation density crystals have been identified and optimized for multicrystalline silicon growth (such as minimizing stress by maintaining a flat solid/liquid interface and controlling cooling conditions, and allowing favorable nucleation conditions), the actual mechanisms for dislocation generation in multicrystalline silicon have not been extensively studied, though they have a strong impact on the solar cell efficiency. By examining defect-etched wafers from the entire ingot height, we have shown [20] that the columnar dislocation clusters that dominate in this material all originate, either at grain boundaries, or from a region below the lowest part examined. Furthermore, from the constant absolute position of the clusters versus the relative movement of the grain boundaries as a function of height, it was concluded that the dislocation clusters were nucleated and developed by multiplication very close to the solid/liquid interface, probably being affected by the image forces of the surface, thus the dislocation activities appear to occur at very high temperatures, close to the melting point of silicon.

A second study, of the dislocation evolution at the very bottom of an ingot, showed that initially the bulk of the crystal was virtually devoid of dislocations, and that even the dislocations from the bottom originated at grain boundaries [21], see Fig. 1. Furthermore, it was observed that dislocation generation occurs at special CSL grain boundaries, and at localized positions on these boundaries, probably corresponding to local faults, which act as stress concentrators necessary to locally increase the relatively low stress levels occurring during crystal growth to the high levels required for dislocation nucleation. This has been
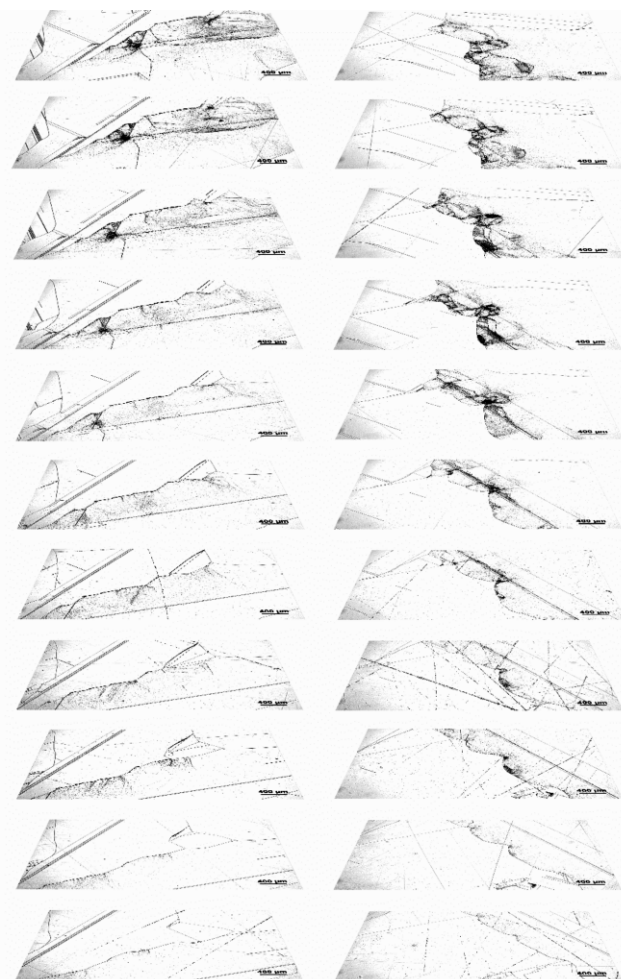

Figure 1 Illustration of dislocation density development in the bottom of an ingot, taken from Ref. [21].

substantiated by further investigations of special junctions at Σ27a CSL grain boundaries [22].

A last, important observation about dislocation clusters is that they tend to organize in structures perpendicular to slip planes [20] (as shown in Fig. 2) which is remarkable since in most studies, such ordered dislocation structures are interpreted as slip lines, i.e. a trace of the movement of the dislocations. Transmission electron microscopy (TEM) observations of such structures [23] clearly showed that these structures are not slip lines, and that the dislocations have moved perpendicular to the lines and aligned in order to reduce the stored energy of the plastic deformation, i.e. a *recovery* process. These mechanisms necessarily also happen at very high temperatures because of the high activation energy of the dislocation climb, a movement mode necessary for organizing these structures.

The important conclusion from these observations is that since most of the foundations of the structure happen at a very early stage, during nucleation or shortly after the solidification, it is necessary to focus the attention to
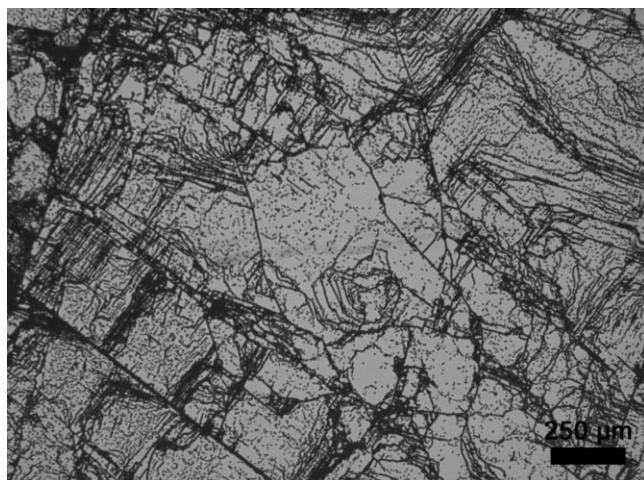
Figure 2 Commonly observed dislocation etch-pit pattern showing dislocation alignment caused by recovery.

improve crystallization conditions rather than attempting to improve the structure postcrystallization.

3 Improved crystallization methods Crystallization is one of the first steps during the silicon solar-cell value chain. Before silicon solar cells are processed, a silicon ingot is grown either by monocrystalline processes (the most commonly used is the Czochralski (CZ) process) or by multicrystalline (mc) processes (in Bridgman-type, directional solidification, furnaces). As previously mentioned, currently a large share of the world solar cells is produced by multicrystalline processes and the aim is to achieve similar energy conversion efficiencies as the monocrystalline cells. Control of the nucleation during directional solidification of silicon allows to controlling the structure development in the final ingot. Many research works have been devoted to study and understand the solidification mechanisms [2, 24]. In particular, research works have proposed new methods of crystallization to achieve high efficiency solar cells. Stoddard et al. [25] presented a new technique (quasi-mono) for casting ingots with the potential for producing silicon with extremely low defects densities. They produced $156 \times 156 \, cm^2$ size solar cells with efficiencies up to 17% using industrial screen-print processes. They also indicated that the silicon ingots produced by this method may have lower concentration of metallic impurities due to a more efficient segregation when few grain boundaries and dislocations are present in the material [25]. It is also expected that the quasi-mono process would give ingots with lower oxygen content than the CZ process. Furthermore, the production throughput of this type of casting processes is 3–5× higher than for a CZ puller [25], thus it can have huge economical consequences. Several industrial producers of multicrystalline silicon have since then adopted methods to produce similar material via controlled seeding.

Dendritic casting is another method that has been proposed to produce silicon ingots for solar cells with high

efficiencies. This method was developed by Fujiwara et al. [26]. It is based on inducing a dendrite growth in the initial stage of directional solidification by applying high undercooling close to the crucible bottom at the start of crystallization. They found that the growth direction of these dendrite crystals was $\langle 112 \rangle$ or $\langle 110 \rangle$, constrained to run parallel to the crucible bottom, and the orientation of the upper surface of each dendrite crystal was (110) or (112), respectively [26]. The solar cells taken from the middle of the ingot made by this method had higher efficiency (about 1% absolute) than the standard methods [26]. In addition to these, other methods have been proposed in recent years [27].

Many studies in this direction have also been carried out at NTNU where principles of "*structure-control*" (grain size and orientation) have been applied to multicrystalline (mc) silicon ingots made in a pilot-scale directional solidification furnace. Nucleation and growth at high undercooling were applied during crystallization of solar-cell silicon ingots. Two mc Si ingots of 250 mm diameter and approximately 100 mm height were cast in a pilot-scale furnace (Crystalox 250). This furnace consists of a graphite support ring and support plate, a susceptor, carbon fiber insulation and a variable heat leak (VHL). The VHL system, which is located underneath the crucible, allows for adjusting the heat flow through the bottom of the crucible. The same type of feedstock, crucible and coating materials were used to produce two ingots. Both were doped with the same amount of boron in order to produce p-type materials with the same resistivity. To obtain forced cooling of the silicon melt in the first casting experiment (B1), the VHL was quickly opened just before nucleation started. More details about the experimental work can be found in Ref. [28]. Two slices taken from the center of the two ingots were selected for analysis and characterization. Figure 3 shows an optical micrograph of the ingot with high initial cooling rate (B1). This ingot (B1) had an abnormally large twinned grain extending over nearly the whole section while the second
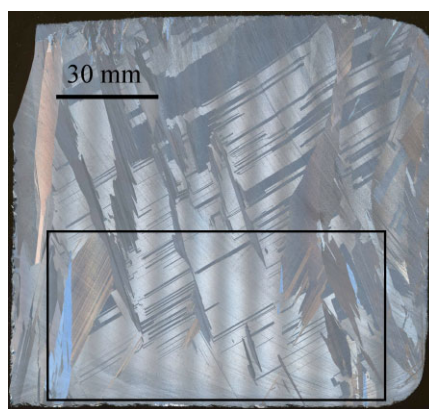

Figure 3 (online color at: www.pss-a.com) Optical micrograph of a cross section of the ingot with high initial cooling rate (B1). The rectangular area shows the area selected for electron backscattered diffraction (EBSD) map.

Phys. Status Solidi A 210, No. 4 (2013)

Feature
Article

645

ingot (B2) had many small grains, which is typical for mc Si ingots produced with a standard cooling rate. Figure 4 shows an EBSD micrograph of the grain orientation of a section from the ingot with the high initial cooling rate (B1). Clearly, there is one large twinned grain (blue/pink) with a growth direction close to ⟨112⟩. The minority carrier lifetime measurements by quasi-steady-state photoconductance showed that the ingot with the high initial cooling rate (B1) has higher lifetime than the ingot with standard cooling rate (B2). The lifetime of the large twinned grain in the ingot B1 was approximately 28 μs, while it was approximately 18 μs for B2. The minority carrier diffusion length (measured by surface photovoltage measurements) of ingot B1 was observed to be significantly longer than in B2, with a maximum of approximately 250 and 180 μm, respectively.

These results show that there is a potential of increasing the electrical properties of the final solar-cell device by this structure-control method. Other studies at NTNU have been performed on nucleation of silicon on Si_3N_4-coated SiO_2 crucibles [29]. They have indicated that the coating thickness, oxygen concentration, wetting angle or roughness of the coating do not affect the undercooling at a given cooling rate [29]. The same author [30] has recently shown that the cooling rate has a significant influence on the grain size of multicrystalline silicon ingots. The samples with the lowest cooling rate (10 K min^{-1}) were dominated by one or few large grains, while the samples with the higher cooling rate (30 K min^{-1}) had a more uniform and smaller grain distribution [30]. This indicates that the highest cooling rate gives the higher nucleation rate [30].

Furthermore, numerical modelling has been used to optimize crystallization processes for solar-cell silicon. An extensive work in this direction has been done by the simulation group at SINTEF (a research center closely working with the university) and NTNU. Bellmann and Meese [31] have reported on the effect of the steady crucible rotation on the melt flow and impurity segregation. They showed that low rotation rates at 1–2 rpm increased the radial segregation in the first half period of solidification, while an opposite behavior was observed for the second half period of solidification. Here, radial segregation was increased at high rotation rates (from 3 to 5 rpm) with small impact at 1–2 rpm [31]. The same group also studied the effect of the shape of the solidification front on the flow pattern and impurity distribution in mc silicon ingots [32]. They found that when the solidification occurs with a planar solid/liquid interface, the flow intensity is low and the impurity segregation is diffusion-controlled and nearly uniform in the radial direction [32]. With a concave interface the flow intensity is one order of magnitude higher and the radial impurity segregation increases [32].

Impurity distribution is also an important research area at NTNU. As previously mentioned, impurity segregation and precipitation are detrimental to the electrical properties of the solar-cell device. Some of the most detrimental impurities (such oxygen, iron and chromium) have been extensively studies at NTNU. Kvande et al. [33] showed that at slow cooling rates mc silicon ingots have higher oxygen concentration and lower minority carrier lifetime. The effect of oxygen on a new generation of silicon feedstock materials, named UMG (upgraded metallurgical grade), was investigated by Di Sabatino et al. [34]. They showed the effect of heat treatments to reduce and control the oxygen distribution on mc silicon ingots for solar cells. A solar cell efficiency reduction by 1–3% absolute value was estimated on ingots made from UMG feedstock with high oxygen concentration [34]. Iron and chromium are fast diffusing impurities in silicon and introduce allowed energy states close to the middle of the silicon bandgap. Both Fe and Cr have been shown to dramatically reduce the minority carrier lifetime in the grown mc Si ingots ([35] and [36], respectively). However, the phosphorous gettering step, during standard solar-cell processing, helps to retain some of the electrical properties. Hystad et al. [36] and Saynova et al. [37] reported that the minority carrier lifetime after P gettering was increased by two orders of magnitude in mc silicon solar cells contaminated with Cr. Recently, Coletti et al. [38] have well summarized the current knowledge about impurities in silicon solar cells. However, research still needs to be addressed to completely understand the fundamental mechanisms of impurity contamination and the interaction with other defects (such as grain boundaries and dislocations) in mc silicon.

4 Combining characterization techniques Investigation of defects and defects formation as well as the effect of crystallization parameters of mc silicon for solar cells requires the access to advanced characterization tools. A large part of the research activities at NTNU is based on characterization and is devoted to development of advanced characterization tools. Research on photovoltaics often involves several aspects, e.g. physics, chemistry, etc. Advanced characterization tools should then be used in combination to study in depth the silicon materials and their properties. In this section we show some examples of our work in this field.
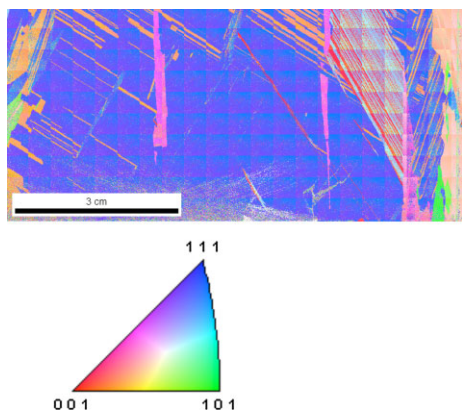

Figure 4 (online color at: www.pss-a.com) EBSD micrograph of a selected area of ingot B1 with inverse pole figure.

In order to study impurity distribution in solar-cell silicon it is important to have access to analytical tools that allow us to measure the impurity concentrations with high accuracy. The levels of impurities are often in the low-ppb range, thus these measurements are not straightforward. We have measured the impurity concentration in our mc silicon ingots by glow discharge mass spectrometry (GDMS) [39] and combined these measurements with other advanced techniques, such as Fourier transform infrared spectroscopy (FTIR) and Hall mobility measurements. Recently, Modanese et al. [40] developed a method to calculate the net doping density in compensated mc Si ingots. They compared four-point-probe resistivity measurements with GDMS measurements showing a good agreement [40]. A combination of GDMS, resistivity and a method based on minority carrier lifetime measurements also showed a good agreement between these three techniques [41]. In particular, the GDMS measurements and the lifetime measurement were useful to calculate the concentration of carriers in solar-cell silicon [41]. Minority carrier lifetime measurements by microwave photoconductance decay (μ-PCD) before and after light soaking were used to dissociate the FeB pairs, and then to determine the B content. Also, impurity measurements by GDMS have been combined with Hall mobility measurements to improve our understanding of the role of dopants in compensated materials and the effect of majority carrier mobility [42].

In another investigation carried out at NTNU, GDMS was used to detect and quantify the amount of impurities present in an upgraded metallurgical-grade silicon feedstock material. Dislocation density analysis and minority carrier lifetime measurements were carried out to select areas of the ingot with poor electrical properties. These areas were further investigated by state-of-the-art transmission electron microscopy (TEM) techniques. It was shown that these areas of low lifetime were decorated with Cu–Ni–Fe silicides and oxygen complexes. Most of the metal precipitates were found at grain boundaries. Figure 5 shows TEM bright-field images and energy-dispersive spectroscopy (EDS) maps showing the Cu and Ni precipitates. More details about this study can be found in Ref. [43]. As indicated in the previous section, the study of defects in mc silicon is not straightforward. Thus, a combination of electron back-scattered diffraction (EBSD) by scanning electron microscopy (SEM), electron-beam-induced current (EBIC) and TEM was performed to investigate the effect of grain boundaries and the recombination activity of precipitated impurities in multicrystalline silicon wafers. Figure 6a and b shows the EBIC and EBSD maps of the same area of a mc-Si wafer. Note that some grain boundaries correspond to the high contrast lines in the EBIC map. The darkest lines correspond to the highest recombination regions. Different grain boundaries have different recombination activity. The TEM analysis taken from one of the grain boundaries with the highest EBIC contrast (Fig. 6c) shows the presence of many SiOx precipitates along the boundary, thus explaining
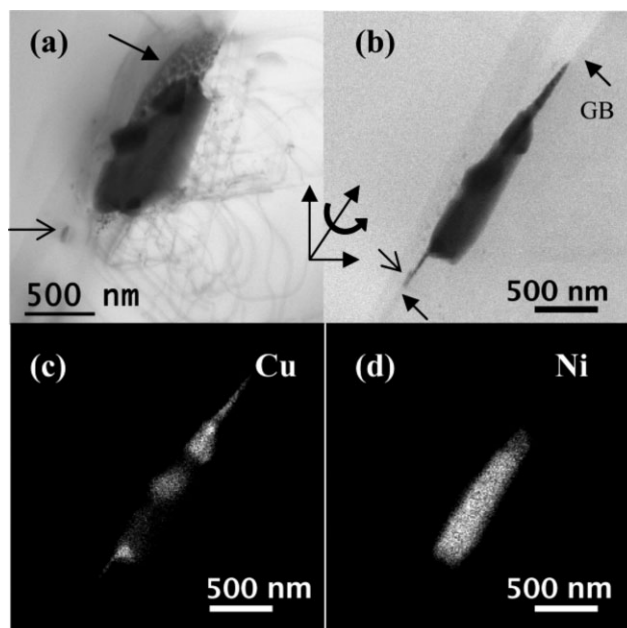

Figure 5 (a) Transmission electron microscopy (TEM) bright-field image; (b) scanning transmission electron microscopy (STEM) bright-field image. EDS elemental maps from the same cluster show that, in addition to silicon, the main constituents are copper (c) and nickel (d).
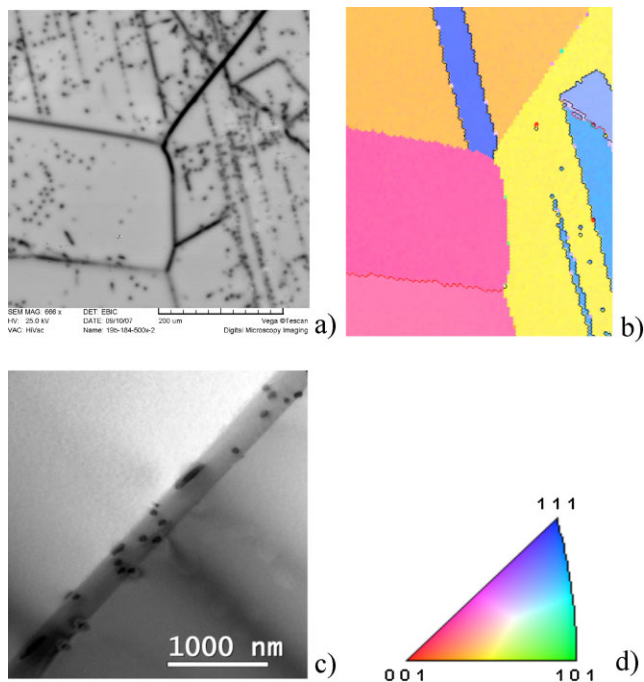

Figure 6 (online color at: www.pss-a.com) (a) Electron-beam-induced current (EBIC) and (b) corresponding EBSD maps of a mc-Si wafer; (c) TEM micrograph of selected area of the same wafer; (d) inverse pole figure.

why this boundary had the highest recombination activity among the investigated boundaries. Furthermore, it was shown that subgrain boundaries were recombination active; this small-angle grain boundary ($<5°$) was not evident in the EBSD maps. This corresponds well with other studies of electrical activity of subgrain boundaries, e.g. Ref. [6]. More details about this study can be found in Refs. [44, 45].

5 Concluding remarks We have reviewed some of the research work on solar-cell silicon materials. In particular, we have reported on the recent state-of-the-art research activities at NTNU on defects, crystallization and characterization.

Control of nucleation and growth during the crystallization of the silicon ingots allows for control of the materials structure development. We have shown that high initial cooling rate can give ingots with larger grains and preferred crystal orientation. Such control of nucleation conditions, although difficult to achieve in practice, appears to be a very important prerequisite for producing low defect density materials and, hence, high-performance solar cells.

Combination of advanced characterization tools allows for an indepth study of materials properties. In particular, combination of techniques is important in order to tailor the investigation from the macro- to the microscale.

References

[1] G. Hering, Photon Int. **3**, 132 (2012).

[2] L. Arnberg, M. Di Sabatino, and E. Øvrelid, J. Cryst. Growth **360**, 56–60 (2012).

[3] T. Buonassisi, A. A. Istratov, D. Pickett, M. A. Marcus, T. F. Ciszek, and E. R. Weber, Appl. Phys. Lett. **89**, 042102 (2006).

[4] A. Garg, W. A. T. Clark, and J. P. Hirth, Philos. Mag. A **59**, 479 (1989).

[5] A. Voigt, E. Wolf, and H. P. Strunk, Mater. Sci. Eng. B **54**, 202 (1998).

[6] J. Chen and T. Sekiguchi, Jpn. J. Appl. Phys. Part 1 **46**, 6489 (2007).

[7] D. Hull and D. J. Bacon, Introduction to Dislocations (Elsevier, Amsterdam, 2011).

[8] H. Alexander and P. Haasen, Dislocations and Plastic Flow in the Diamond Structure, Vol. 22 (Academic Press, New York, 1969).

[9] H. Behnken, in: Proc. 24th European Photovoltaic Solar Energy Conference, Hamburg, Germany, 2009, pp. 1281–1285.

[10] M. M'Hamdi and E. Olsen, Proceedings of 21st EU-PVSEC (2006).

[11] S. Nakano, X. J. Chen, B. Gao, and K. Kakimoto, J. Cryst. Growth **318**, 280 (2011).

[12] M. Kittler, W. Seifert, and K. Knobloch, International Conference on Electronic Materials ICEM, Xiàn, China, 2002.

[13] V. Kveder, M. Kittler, and W. Schroter, Phys. Rev. B **63**, 115208 (2001).

[14] A. Bentzen, A. Holt, R. Kopecek, G. Stokkan, J. S. Christensen, and B. G. Svensson, J. Appl. Phys. **99**, 93509-1 (2006).

[15] M. Rinio, S. Peters, M. Werner, A. Lawerenz, and H. J. Möller, Solid State Phenom. **82–84**, 701 (2002).

[16] C. Donolato, J. Appl. Phys. **84**, 2656 (1998).

[17] G. Stokkan and T. Brynjulfsen, in: Proceedings CSSC-4, Taipei, Taiwan, 2010.

[18] G. Stokkan, Acta Mater. **58**, 3223 (2010).

[19] K. Fujiwara, W. Pan, N. Usami, K. Sawada, M. Tokairin, Y. Nose, A. Nomura, T. Shishido, and K. Nakajima, Acta Mater. **54**, 3191 (2006).

[20] B. Ryningen, G. Stokkan, M. Kivambe, T. Ervik, and O. Lohne, Acta Mater. **59**, 7703 (2011).

[21] I. Odland and G. Stokkan, in: Proc. 4th International Workshop on Crystalline Silicon Solar Cells (CSSC 4), Taipei, Taiwan, 2010 pp.

[22] T. Ervik, M. Kivambe, G. Stokkan, B. Ryningen, and O. Lohne, in: Proc. 26th European Photovoltaic Solar Energy Conference and Exhibition, Hamburg, Germany, 2011 (WIP-Munich), pp. 1895–1899.

[23] M. M. Kivambe, G. Stokkan, T. Ervik, B. Ryningen, and O. Lohne, J. Appl. Phys. **110**, 063524 (2011).

[24] L. Arnberg, M. Di Sabatino, and E. Øvrelid, Trans. Indian Inst. Met.; DOI: 10.1007/s12666-012-0165-2 (2012).

[25] N. Stoddard, B. Wu, I. Witting, M. Wagener, Y. Park, G. Rozgonyi, and R. Clark, Solid State Phenom. **131–133**, 1 (2008).

[26] K. Fujiwara, W. Pan, N. Usami, and K. Nakajima, J. Cryst. Growth **292**, 282 (2006).

[27] K. Fujiwara, Int. J. Photoenergy **2012**, DOI: 10.1155/2012/169829.

[28] M. Di Sabatino, M. Juel, L. Arnberg, M. Syvertsen, and G. Tranell, Trans. Indian Inst. Met. **62**, 511 (2009).

[29] I. Brynjulfsen, A. Bakken, M. Tangstad, and L. Arnberg, J. Cryst. Growth **312**, 2404 (2010).

[30] I. Brynjulfsen, K. Fujiwara, N. Usami, and L. Arnberg, J. Cryst. Growth **356**, 17–21 (2012).

[31] M. P. Bellmann and E. A. Meese, J. Cryst. Growth **333**, 1 (2011).

[32] M. P. Bellmann and M. M'Hamdi, J. Cryst. Growth, DOI: 10.1016/j.jcrysgro.2011.10.055 (2012).

[33] R. Kvande, Ø. Mjøs, and B. Ryningen, Mater. Sci. Eng. A **413–414**, 545 (2005).

[34] M. Di Sabatino, S. Binetti, J. Libal, M. Acciarri, H. Nordmark, and E. J. Øvrelid, Sol. Energy Mater. Sol. Cells **95**, 529 (2011).

[35] R. Kvande, L. J. Geerligs, G. Coletti, L. Arnberg, M. Di Sabatino, E. J. Øvrelid, and C. C. Swanson, J. Appl. Phys. **104**, 064905 (2008).

[36] M. Hystad, C. Modanese, M. Di Sabatino, and L. Arnberg, Sol. Energy Mater. Sol. Cells **103**, 140 (2012).

[37] D. Saynova, G. Coletti, M. Di Sabatino, and L. J. Geerligs, in: Proc. 25th EUPVSEC, Valencia (Germany), 2010, pp. 1934–1938.

[38] G. Colettti, P. C. P. Bronsveld, G. Hahn, W. Warta, D. Macdonald, B. Ceccaroli, K. Wambach, N. Le Quang, and J. M. Fernandez, Adv. Funct. Mater. **21**, 879 (2011).

[39] M. Di Sabatino, A. L. Dons, J. Hinrichs, and L. Arnberg, Spectrochim. Acta B **66**, 144 (2012).

[40] C. Modanese, M. Di Sabatino, A.-K. Soiland, and L. Arnberg, Phys. Status Solidi C **8**, 713 (2011).

[41] D. Macdonald, F. Rougieux, A. Cuevas, B. Lim, J. Schmidt, M. Di Sabatino, and L. J. Geerligs, J. Appl. Phys. **105**, 093704 (2009).

[42] C. Modanese, M. Acciarri, S. Binetti, A.-K. Soiland, M. Di Sabatino, and L. Arnberg, Prog. Photovolt., DOI: 10.1002/pip.2223 (2012).

[43] H. Nordmark, M. Di Sabatino, E. J. Øvrelid, J. C. Walmsley, and R. Holmestad, EUPVSEC (2007).

[44] S. Binetti, J. Libal, M. Acciarri, M. Di Sabatino, H. Nordmark, E. J. Øvrelid, J. C. Walmsley, and R. Holmestad, Mater. Sci. Eng. B **159-160**, 274, (2009).

[45] H. Nordmark, M. Di Sabatino, M. Acciarri, J. Libal, S. Binetti, E. J. Øvrelid, J. C. Walmsley, and R. Holmestad, 33rd IEEE Photovoltaic Specialists Conference San Diego (CA), USA, May 2008.